Geoderma 335 (2019) 78–87

Contents lists available at ScienceDirect

Geoderma

journal homepage: www.elsevier.com/locate/geoderma

Mapping upland peat depth using airborne radiometric and lidar survey data

Gatis N.[a,*], Luscombe D.J.[a], Carless D.[a], Parry L.E.[b], Fyfe R.M.[c], Harrod T.R.[d], Brazier R.E.[a], Anderson K.[e]

[a] Geography, University of Exeter, Rennes Drive, Exeter, Devon EX4 4RJ, UK
[b] University of Glasgow, Rutherford/McCowan Building, Crichton University Campus, Dumfries, DG1 4ZL, UK
[c] University of Plymouth, Drake Circus, Plymouth, Devon PL4 8AA, UK
[d] Independent Scholar, UK
[e] Environment and Sustainability Institute, University of Exeter Penryn Campus, Penryn, Cornwall TR10 9FE, UK

ARTICLE INFO

Handling Editor: Yvan Capowiez

Keywords:
Gamma-ray attenuation
LiDAR
Remote sensing
Peat depth
Soil organic carbon
Peatland

ABSTRACT

A method to estimate peat depth and extent is vital for accurate estimation of carbon stocks and to facilitate appropriate peatland management. Current methods for direct measurement (e.g. ground penetrating radar, probing) are labour intensive making them unfeasible for capturing spatial information at landscape extents. Attempts to model peat depths using remotely sensed data such as elevation and slope have shown promise but assume a functional relationship between current conditions and gradually accrued peat depth. Herein we combine LiDAR-derived metrics known to influence peat accumulation (elevation, slope, topographic wetness index (TWI)) with passive gamma-ray spectrometric survey data, shown to correlate with peat occurrence, to develop a novel peat depth model for Dartmoor.

Total air absorbed dose rates of Thorium, Uranium and Potassium were calculated, referred to as radiometric dose. Relationships between peat depth, radiometric dose, elevation, slope and TWI were trained using 1334 peat depth measurements, a further 445 measurements were used for testing. All variables showed significant relationships with peat depth. Linear stepwise regression of natural log-transformed variables indicated that a radiometric dose and slope model had an r^2 = 0.72/0.73 and RMSE 0.31/0.31 m for training/testing respectively. This model estimated an area of 158 ± 101 km^2 of peaty soil > 0.4 m deep across the study area. Much of this area (60 km^2) is overlain by grassland and therefore may have been missed if vegetation cover was used to map peat extent. Using published bulk density and carbon content values we estimated 13.1 Mt. C (8.1–21.9 Mt. C) are stored in the peaty soils within the study area. This is an increase on previous estimates due to greater modelled peat depth. The combined use of airborne gamma-ray spectrometric survey and LiDAR data provide a novel, practical and repeatable means to estimate peat depth with no *a priori* knowledge, at an appropriate resolution (10 m) and extent (406 km^2) to facilitate management of entire peatland complexes.

1. Introduction

The inclusion of wetland drainage and rewetting in the United Nations Framework Convention on Climate Change (2012) has raised renewed interest in mapping peatland extents and depths; to provide better estimates of carbon stocks, monitor changes to peatlands and facilitate appropriate management (Aitkenhead, 2017; Biancalani and Avagyan, 2014). Moreover, it has been recognised that peatlands provide a range of ecosystem services (Grand-Clement et al., 2013) many of which are regulated throughout the full thickness of the peat - in particular, fresh water provision and climate regulation. As blanket peatlands are highly variable in depth (Bragg and Tallis, 2001) there exists an operational challenge to map peat depth at a sufficiently fine spatial resolution to capture the small-scale variability that is known to exist in blanket peat depth (cm's – m's) over the required spatial extents (m's – km's).

The two main methods currently used to measure peat depth are manual probing of the peat *in situ* and ground-penetrating radar (GPR). Peat probing is the more commonly deployed method due to its low cost and minimal equipment requirements (Akumu and McLaughlin, 2014; Beilman et al., 2008; Buffam et al., 2010; Holden and Connolly, 2011; Householder et al., 2012; Parry et al., 2012). Manual probing

* Corresponding author.
E-mail addresses: N.Gatis@exeter.ac.uk (N. Gatis), D.J.Luscombe@exeter.ac.uk (D.J. Luscombe), D.Carless@exeter.ac.uk (D. Carless), Lauren.Parry@glasgow.ac.uk (L.E. Parry), ralph.fyfe@plymouth.ac.uk (R.M. Fyfe), R.E.Brazier@exeter.ac.uk (R.E. Brazier), Karen.Anderson@exeter.ac.uk (K. Anderson).

https://doi.org/10.1016/j.geoderma.2018.07.041
Received 23 February 2018; Received in revised form 23 July 2018; Accepted 27 July 2018
0016-7061/ © 2018 The Authors. Published by Elsevier B.V. This is an open access article under the CC BY license (http://creativecommons.org/licenses/BY/4.0/).

entails pushing a thin (~1.5 cm diameter) metal pole into the peat, at discrete spatial intervals, until resistance from the underlying soil/bedrock is felt. These point measurements are then commonly interpolated across large sites to produce peat-depth models (for examples see Akumu and McLaughlin, 2014; Householder et al., 2012). In contrast, GPR is a non-invasive proximal sensing technique whereby the two-way travel time of a pulse of high frequency energy reflected off the interface between the saturated peat and the underlying strata is measured (Davis and Annan, 1989). This delivers fine spatial resolution (mm to cm) measurements of peat thickness every 0.5 to 1 m along a transect typically tens to hundreds of meters in length (e.g. Comas et al., 2015; Lapen et al., 1996; Parry et al., 2014; Plado et al., 2011). A series of transects can then be interpolated to produce a peat depth map. Both probe and GPR measurements are labour intensive particularly when mapping peat depth over landscape extents, for example Parsekian et al. (2012) took 53 person hours to probe 0.095 km^2 on a 20 m grid and 30 person hours to cover the same area using GPR. Resultantly, the scale of blanket peat coverage across Dartmoor, UK (406 km^2) would preclude the use of both of these methods.

As an alternative to measuring peat depth *in situ,* some studies have modelled peat depth using remotely sensed data. Holden and Connolly (2011) modelled peat depth for the Wicklow mountains, Ireland using an exponential relationship with slope constrained by elevation (national DTM) and disturbance mapped using satellite imagery. Parry et al. (2012) also used exponential relationships with airborne Interferometric Synthetic Aperture Radar derived slope and/or elevation, this time constrained by previously mapped soil/vegetation units to model peat depth for Dartmoor. Rudiyanto et al. (2016) used Shuttle Radar Topography Mission derived digital elevation model to derive topography, slope, aspect, wetness index and distance to river metrics. They then applied a quantile regression function and cubist regression tree models to model tropical peat depth in Indonesia. In a more recent study of Indonesian tropical peat depths, Rudiyanto et al. (2018) applied machine learning to 37 potential covariates derived from satellite-based remote sensing data. They found elevation, radar images (a proxy for wetness), valley bottom flatness (indicative of areas of deposition) and distance to the nearest river to be the main controls on peat thickness. These models varied in resolution (30 m to 1 km) and coefficient of determination from 0.52 (Parry et al., 2012) to 0.97 (Rudiyanto et al., 2018) all showing the potential of modelling peat depths across larger extents. However, these models do not account for the underlying, and often complex topography commonly smothered by blanket bogs. In addition, they assume a direct relationship between peat depths and present accumulation rates controlled by topography, elevation, slope, aspect and wetness.

Estimates of peat depth are sometimes limited to areas previously defined as peatlands (e.g. Akumu and McLaughlin, 2014; Householder et al., 2012). The extent of which have been delineated by the presence of vegetation communities visible in aerial (e.g. Cruickshank and Tomlinson, 1990) and/or satellite (e.g. Aitkenhead, 2017) imagery. This assumes that peat is overlain by peat-forming vegetation communities, however, where peatlands have been subject to land management, peat may be overlain by non-peat forming vegetation (Connolly et al., 2007). To capture both actively forming and relic peats, it is imperative that any method to map peat depths are capable of including these areas of peat overlain by non-peat forming vegetation.

An emerging remote sensing method that has shown potential to map peat depth over landscape extents is airborne gamma-ray spectrometric survey. Gamma-ray spectrometers measure in the range 0.2 to 3 MeV, equivalent to a wavelength of 3×10^{-12} m, for geological interest (Minty, 1997). Potassium (K), Uranium (U) and Thorium (Th) in rocks and soils have naturally occurring radioisotopes (and daughter isotopes) that release gamma-rays with characteristic energy and intensity which can be detected by such airborne gamma-ray spectrometers (Minty, 1997). Radiation emitted from the underlying bedrock is attenuated (mostly incoherent scattering) by the overlying soils, the amount of attenuation is dependent on the thickness of the soil, porosity, saturation and density (Beamish, 2013a). Rawlins et al. (2009) noted the remarkably high absorbance of naturally occurring potassium by peatland soils in Northern Ireland. Using the same data, the extent to which total K, U and Th can be used to map peat was investigated by Beamish (2013a). He then extended this work to other areas in the UK comparing areas of mapped peat to radiometric dose (total P, U and Th) (Beamish, 2015, 2013b) noting considerable variation within a peatland. However, due to the high attenuation by saturated peat (90% of radiation attenuated by 60 cm of 80% saturated peat) the ability of radiometric data to map peat depth has been questioned (Beamish, 2013b). Despite this Keaney et al. (2013) showed the potential of radiometric data to update existing peat depth models by comparing the spatial patterning of airborne radiometric data to that of probed peat depths for a blanket bog and a lowland raised bog in Northern Ireland.

Herein we combine LiDAR derived metrics known to influence peat accumulation (elevation, slope, topographic wetness) with gamma-ray spectrometric survey data, shown to correlate with peat occurrence to investigate whether using two technologies (LiDAR and gamma-ray spectroscopy) with differing data content can be used more effectively in tandem to develop a novel peat depth model for Dartmoor.

2. Material and method

2.1. Study area

Dartmoor National Park lies in the southwest of England (Fig. 1a), it contains an extensive area of upland moor. Its maritime location and elevation (reaching 623 m above sea level) result in average annual precipitation of 1974 mm and a mean monthly temperature range of 0.8 to 17.7 °C. These conditions enable blanket bog, a globally restricted, and consequently important, habitat to form (Lindsay, 1995; Tallis, 1997). The area is also important regionally for drinking water provision and flow regulation as Dartmoor contains the headwaters of many rivers. The peatland not only stores carbon but also paleoarchaeological records (e.g. Fyfe and Woodbridge, 2012) and in some locations heritage assets e.g. burial cists (Jones, 2016) as well as providing ecosystem services (Millennium Ecosystem Assessment (https://www.millenniumassessment.org/en/index.html) including regulation (e.g. climate) and cultural (e.g. recreational (Liston-Heyes and Heyes, 1999)). A strong body of previous work documenting peat depth surveys across parts of Dartmoor can be found in (Fyfe et al., 2014, 2010; Fyfe and Woodbridge, 2012; Harrod, 2016; Parry, 2011; Parry et al., 2014; Parry and Charman, 2013), data from some of these surveys were available to this study.

The survey area (Fig. 1b) (406 km^2) consists of moorland overlying the impermeable but locally fractured granite batholith of Dartmoor. All bedrock materials emit radionuclides which can be monitored by airborne gamma-ray spectrometry however, the radiometric signal varies with bedrock type (Rawlins et al., 2007). In order to minimise variability in radiogenesis from the underlying bedrock the survey area was restricted to the granite and microgranite bedrocks, delineated by the 1:50000 bedrock geology map (British Geological Survey, 2016).

2.2. Radiometric dose

Airborne gamma-ray spectrometric data in the energy range 0.40–2.81 megaelectron volts (Beamish et al., 2014) were collected by the NERC Tellus project in summer and autumn 2013. These data were downloaded for use in this research from http://www.tellusgb.ac.uk/Data/airborneGeophysicalSurvey.html. Following Beamish et al. (2014) the air absorbed radiometric dose (D) (nGy·h^{-1}; nanoGray per hour) was calculated using Eq. (1).

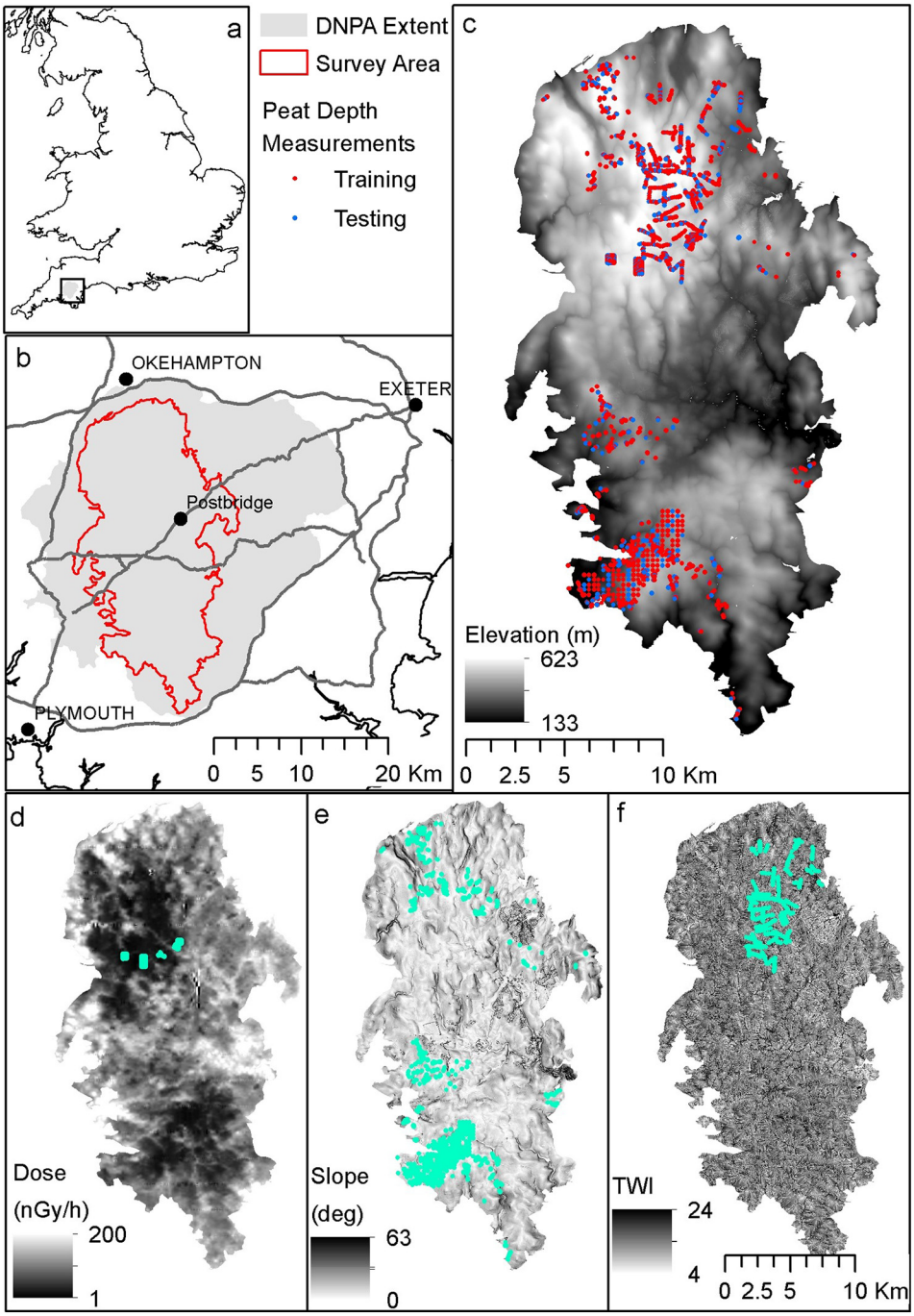

Fig. 1. Location and extent of Dartmoor National Park Authority (DNPA) within Southwest England (a). Location of study area within Dartmoor National Park (b). Location of peat depth measurements by peat probe (Harrod, 2016; Parry et al., 2012) and ground penetrating radar (Fyfe et al., 2014, 2010) within survey area overlying elevation (m) (derived from LiDAR) (c). Radiometric dose ($nGy\,hr^{-1}$) (derived from gamma-ray spectrometric survey) and location of peat depth measurements by Fyfe et al. (2014, 2010) (d), slope (°) and location of peat depth measurements by Parry et al. (2012) (e) and topographic wetness index (TWI) (dimensionless) (derived from LiDAR) and location of peat depth measurements by Harrod (2016) (f).

$$D\ (nGy{\cdot}h^{-1}) = 13.078\ K + 5.675\ U + 2.494Th \quad (1)$$

where K is the corrected potassium (%) and U and Th the corrected uranium and thorium (ppm). Dose rather than individual radionuclides were used to increase the signal to noise ratio. Dose (a measure of energy recorded by the sensor) was used rather than total counts (events detected) as it is not detector specific. All analyses were carried out using ArcGIS (v10.0, ESRI, Redlands, California, USA). The unevenly spaced (60–70 m along North-South trending track, 200 m across track) point data were interpolated to a 10 m grid using a spline interpolation (minimum curvature gridding), an interpolation method recommended for anisotropic geophysical data (Erdi-Krausz et al., 2003). A 10 m grid was selected to be equivalent to the location accuracy of the least accurate point peat depth measurements (Section 2.4). The null water level was set at $-6\,nGy{\cdot}h^{-1}$, values below this were deemed to be anomalies due to the interpolation and set to $-6\,nGy{\cdot}h^{-1}$. All the dose values were then increased so the null water level became 1 to enable analysis of exponential and logarithmic relationships.

2.3. Elevation, slope and topographic wetness index

LiDAR data, processed into a digital surface model (DSM) (Ferraccioli et al., 2014) were also collected by the NERC Tellus project in summer and autumn 2013. These data were downloaded from https://catalogue.ceh.ac.uk/documents/b81071f2-85b3-4e31-8506-cabe899f989a. The 1 m resolution LiDAR DSM with average accuracy of 25 cm was aggregated (mean) to a 10 m cell size equivalent to the radiometric dose grid. The digital surface model was used in preference to the digital terrain model as in short sward vegetation, which covers

most of the survey area, the DSM has been shown to effectively represent the underlying topography not the vegetation (Luscombe et al., 2015). In addition, the author's experience of these data suggest the algorithm used to remove the vegetation from the DSM to create the DTM can result in artificial processing artefacts. Slope was derived from the 10 m DSM using the slope function within the spatial analyst toolbox in Arc GIS 10.0. TWI was calculated from a/tanb where a is the upslope contributing area and b is the slope (Beven and Kirkby, 1979). The upslope contributing area was determined using the flow accumulation function within the same toolbox.

2.4. Peat depth

Peat depth measurements (Fig. 1) were compiled from three different sources; Parry et al. (2012) and Harrod (2016) measured peat depth from the surface with a peat probe, whilst Fyfe et al. (2014, 2010) collected peat thickness measurements in four areas focused on thicker peats using ground penetrating radar measurements (GPR). Given the mix of peat depth and peat thickness data (which for practical purposes are equivalent), the term peat depth was selected as this is the term more commonly used by landscape managers and peatland restoration practitioners.

The samples are unevenly distributed across the study area (Fig. 1) which covers very difficult terrain for fieldwork. Parry et al. (2012) collected 1100 probed peat depths, covering a range of vegetation and soil types, of which 1019 lie within the study area. Briefly, an average of five peat depths were taken for each location over 8 m^2 area and assigned to the central point. Fyfe et al. (2014, 2010) collected ground penetrating radar measurements (n = 59,760) focussed on areas known to have the deepest peats using a PulseEkko Pro system with 200 MHz antennae every 0.5 m in step mode along transects. Both the Parry et al. (2012) and Fyfe surveys used a Differential Global Positioning System (GPS) resulting in location accuracies < 0.3 m. Harrod (2016) collected 1936 augured peat depths along 46 transects in the north east of the study area to map soil types. Location data were collected for approximately every 4th measurement (approximately 100 m apart, a total of 487 points) using a handheld GPS, accurate to 10 m.

Peat depth points were spatially averaged, using the point to raster tool with a cell value determined by the mean of all the points within each cell. A 10 m raster was selected to match the spatial resolution of the radiometric dose, elevation, slope and TWI data. To ensure the data were not skewed towards deeper peat due to greater sampling density by GPR, these data were subsampled every 50 m. To investigate subpixel peat depth, variability statistics (mean, maximum, minimum, standard deviation and count) were calculated for the peat depth measurements within each cell.

2.5. Model derivation and validation

A quarter of the data were randomly selected and set aside for validation (n = 445), the remaining training data (n = 1334) were used to derive the peat depth model. Model derivation was carried out using SPSS Statistics for Windows v.23.0 (IBM Corp, Armonk, New York). All variables were natural log-transformed to improve normality. Linear relationships between peat depth, radiometric dose, elevation, slope and TWI were tested. Stepwise multiple linear regression was carried out with depth as the dependent variable and radiometric dose, elevation, slope and TWI as the independent variables.

The relationship between peat depth and the theoretical attenuation of a single homogenous layer comprising soil, air and water (Beamish, 2013a) was also tested by solving Eq. (2).

$$\text{If } R > R_0 \text{ then } D = 0 \text{ Else } D = \frac{\ln\left(R/R_0\right)}{-(P_P.\,\mu_P + P_W.\,\mu_W + P_A.\,\mu_A)} \quad (2)$$

where D was the peat depth (cm) (dependent variable), R the radiometric dose (nGy·h^{-1}) (variable for each cell), R_0 the radiometric dose with no peat cover (nGy·h^{-1}) (not pre-defined and uniform across study area), μ_P, μ_W, μ_A the mass attenuation coefficient (constant) and P_P, P_W, and P_A the proportions (not predefined and uniform across study area) of peat, water and air respectively. The mass attenuation $\mu_P = \mu/\rho$ where μ was the linear attenuation coefficient (an intrinsic property of the material proportional to the total number of electrons per unit volume of the material) and ρ the density. Densities of 0.10 to 0.14 (Parry, 2011 and references therein), 1 and 0.001 gcm^{-3} and linear attenuation coefficients of 0.0528, 0.0572 and 0.0526 $cm^2\,g^{-1}$ were used for peat, water and air respectively. The proportion of peat, water and air were dependent on porosity (0.71 to 0.951) (Rezanezhad et al., 2016) and effective water saturation (variable) as follows: P_P = 1-porosity, P_W = porosity x effective water saturation and P_A = porosity x (1- effective water saturation).

Peat depths were estimated for each grid cell in the survey area, any negative peat depth estimates were set to zero. Negative peat depths occurred where the radiometric dose and slope were both high i.e. in areas where no peat would be expected. The 5 and 95% confidence intervals for peat depth were estimated using the lower and upper bounds for model parameter estimates, the difference of these values was reported as the confidence interval. It was not possible to quantify the uncertainty in slope and radiometric dose so it was assumed they have no uncertainty. This will result in an underestimate of the confidence intervals.

2.6. Carbon stock estimation

Bulk density and carbon content were derived for each grid cell using well-established relationships determined for Dartmoor (Parry and Charman, 2013). Bulk density (gcm^{-3}) = 0.162–0.00214 × depth (m) and carbon content (%) = 49 + 0.874 × depth (m). The carbon content for each pixel (kg C m^{-2}) was estimated by the product of the peat depth, bulk density and carbon content. This was then multiplied by the area of each pixel (100 m^2) to derive the total peat carbon stock. The model was then applied only to the area of peaty soils, > 0.4 m deep with an organic content > 12–18% (Avery, 1980), a commonly used threshold for land management (Joint Nature Conservation Committee, 2011).

The extent and total peat carbon underlying different land covers, as defined by the 1:25000 vector Land Cover Map (Centre for Ecology and Hydrology, 2007), was calculated to assess the usefulness of land cover to map peat extent.

3. Results

3.1. Input data

Fyfe et al. (2014, 2010) targeted areas of blanket bog (Fig. 1d) anticipated to be thicker and found peat depths ranging from 0.61 to 5.91 m. Parry et al. (2012) covered a wider range of peat depths and vegetation types, finding peat depths from 0 to 3.30 m, however this survey did not cover the central portion of Dartmoor (Fig. 1e) where Harrod (2016) found the deepest peats (7.00 m) (Fig. 1f). The number of peat depth measurements in each 10 m^2 grid cell ranged from 1 to 216 and the standard deviation in measured peat depth ranged from 0 to 0.45 m except in one cell where peat depth varied from 2.89 to 5.11 m giving a standard deviation of 1.00 m. Statistics for the peat depths and covariates used in the prediction of peat depth (for the selected 1779 training and testing cells) are provided in Table 1. It can be seen that the training and testing points used did not include the areas with highest radiometric dose, steepest slopes, lowest elevation or greatest TWI (Fig. 1) but did cover the majority of conditions observed.

Table 1
Summary statistics for observed training peat depth data and covariates used in the estimation of peat depth.

Covariates	Description	Unit	Min	Max	Mean	Median	St.dev
Peat depth	Thickness of peat from surface to underlying bedrock.	m	0.0	7.0	117.5	0.58	130.1
Radiometric dose	Total K, U and Th absorbed in air interpolated to a spatial resolution of 10 m	nGy hr^{-1}	4	114	31	26	23
Elevation	DSM with a spatial resolution of 10 m	mASL	222	618	467	486	84
Slope	Rate of change in elevation of surrounding pixels, calculated by ArcGIS slope function	Degrees	0.1	27.7	5.2	4.1	4.1
Topographic wetness index	The ratio of the contributing area and the slope	dimensionless	5.3	18.0	9.5	9.4	1.6

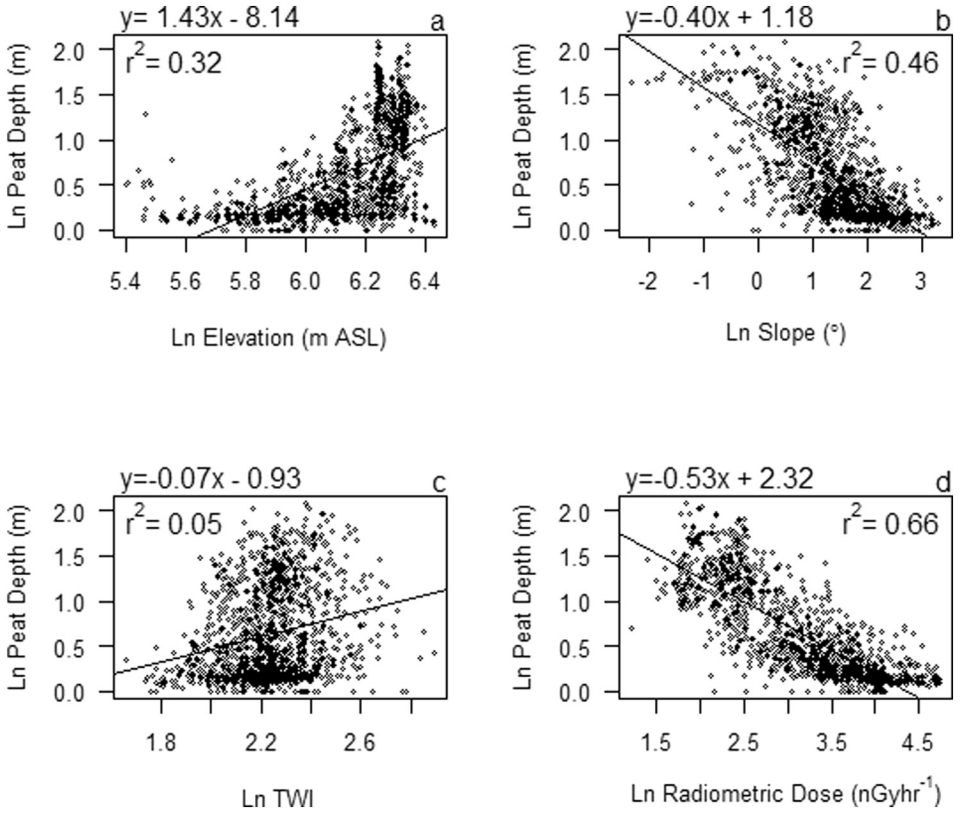

Fig. 2. Relationships between natural log-transformed peat depth (m) and elevation (m) (a), slope (°) (b), wetness (dimensionless) (c) and radiometric dose (nGy hr^{-1}) (d) $p < 0.001$ for all relationships.

3.2. Peat depth model derivation

It can be seen that thinner peat (< 1 m) varied across the range of elevation, slope, TWI and radiometric dose encountered. However, the areas of thickest peats only occurred at higher elevations (Fig. 2a) on flatter slopes (Fig. 2b) where the modelled wetness was greater (Fig. 2c) and had low radiometric dose (Fig. 2d). All four variables had significant relationships with peat depth but the strongest relationship occurred with ln radiometric dose ($r^2 = 0.66$). The theoretical attenuation curve (Eq. (2)) had an r^2 of 0.58 where the theoretical radiation from the bedrock was 45 nGy hr^{-1}, peat porosity (0.79), density (0.10 g cm^{-3}) and effective water saturation of 12%.

Stepwise multiple linear regression (Table 2) indicated that ln radiometric dose was the strongest explanatory variable for peat depth. Adding ln slope as a second covariate increased the r^2 to 0.72 and decreased the RMSE to 0.27 (0.31 m linear scale). The addition of elevation further increased the r^2 but did not reduce the RMSE. It also greatly increased the uncertainty in the modelled result, for example for a radiometric dose of 30 nGy h^{-1}, slope of 5°, and elevation of 460 m the bivariate model predicted a peat depth of 0.63 ± 0.31 m whereas the trivariate model predicted a peat depth of 0.65 ± 4.20 m. For this reason it was decided to use the bivariate (radiometric dose and slope) model. Topographic wetness index had the weakest relationship with peat depth (Fig. 2c) and was not selected by the stepwise multiple linear regression model. It can be seen (Table 2) the testing pixels had similar r^2 and RMSE to the training pixels suggesting the models were appropriate for these data.

Although the plot of modelled against measured peat depth shows good agreement with the 1:1 line (Fig. 3a & c) it can be seen that there is some scatter as the data curves around the line. Modelled peat depth underestimated peat depth for the shallowest and thickest peats and overestimated peat depths for intermediate depths. The plot of residuals against modelled peat depths (Fig. 3b & d) suggests the model is unbiased with no obvious heteroscedasticity. However, it appears that thinner modelled peat depths had positive residuals (underestimation) becoming negative i.e. increasingly overestimating peat depth, with increased modelled depth.

3.3. Modelled peat depth

Modelled areas of deeper peat (linear scale) were concentrated on the higher elevation (Fig. 1c) areas of the north and south moors (Fig. 4a) where the radiometric dose and slope were lower (Fig. 1d & e). Thinner peaty soils (< 0.4 m) were discontinuous moving away from these areas. Mean and median modelled peat depth were 0.50 m and 0.30 m respectively with an interquartile range from 0.08 to 0.67 m

Table 2
Stepwise linear regression results ($p < 0.05$) of natural log-transformed peat depth with natural log-transformed radiometric dose, elevation, slope and topographic wetness index (TWI) as potential explanatory variables. Root mean squared error (m). Values in brackets are for a linear scale.

Model	Variable	Constant	Coefficient	Testing		Training	
				r^2(adj)	RMSE	r^2(adj)	RMSE
1	Ln radiometric dose	2.32	−0.53	0.66 (0.55)	0.30 (0.35)	0.69 (0.59)	0.29 (0.34)
2	Ln radiometric dose	2.19	−0.02	0.72 (0.66)	0.27 (0.31)	0.73 (0.68)	0.27 (0.31)
	Ln slope		−0.18				
3	Ln radiometric dose	0.12	−0.37	0.73 (0.66)	0.27 (0.31)	0.75 (0.69)	0.26 (0.30)
	Ln slope		−0.18				
	Ln elevation		0.31				

with over 99% of modelled depths < 3 m.

The model estimated that peat > 0.4 m thick covers an area of 158 km^2 (99–259 km^2) within the study area (Table 3) storing between 8.1 and 21.9 Mt. C. Most of this peat was overlain by bog (96 km^2) but a considerable proportion was overlain by grassland (60 km^2) (Table 4).

4. Discussion

4.1. Using radiometric dose to estimate peat extent and depth

Theoretically > 0.6 m of saturated peat thickness (equivalent to 0.5 m in a logarithmic scale) will attenuate nearly all of the radionuclides (Beamish, 2013b, Fig. 2) resulting in limited sensitivity to peat thicknesses at greater peat depths than this. This effect can be seen in Fig. 2d where there was a large variation in ln peat depth for a small variation in ln radiometric dose in the range 1 to 3 (equivalent to 1 to 20 nGy h^{-1} in a linear scale). However, ln modelled peat depth shows a strong relationship with ln measured peat depth beyond 0.5 (equivalent to 0.6 m of peat in a linear scale) (Fig. 3c). Keaney et al. (2013) also found radiometric dose to vary with peat depth in the range 2.6 to 8.2 m. Beamish (2015, 2013b, 2013a) interpreted within site peat variation in radiometric dose primarily as variation in effective water

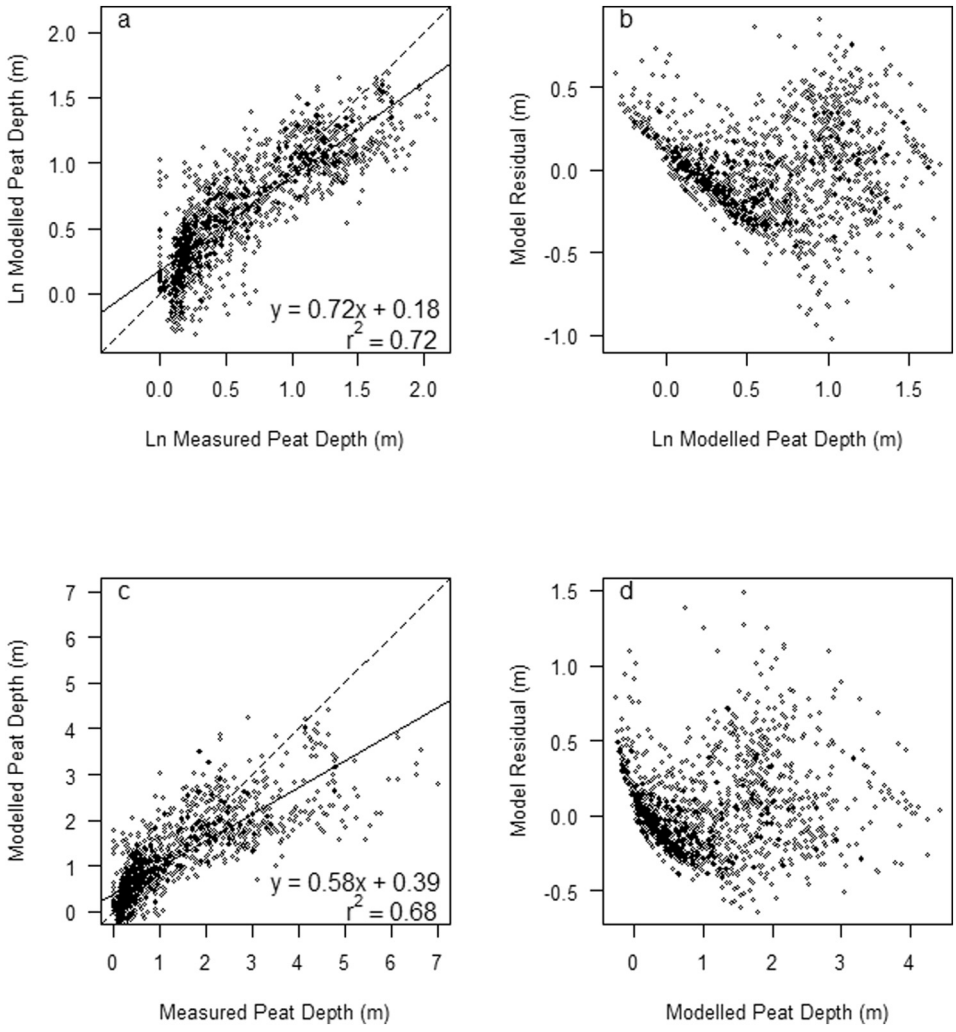

Fig. 3. Relationship between natural log (a & b) and linear (c & d) modelled peat depth (m) and measured peat depth (m) (a & c) as well as modelled peat depth (m) and model residuals (m) (b & d) for a radiometric dose and slope model, coefficients given in Table 2. Linear fit between measured and modelled peat depth (dashed line) and 1:1 line (solid line).

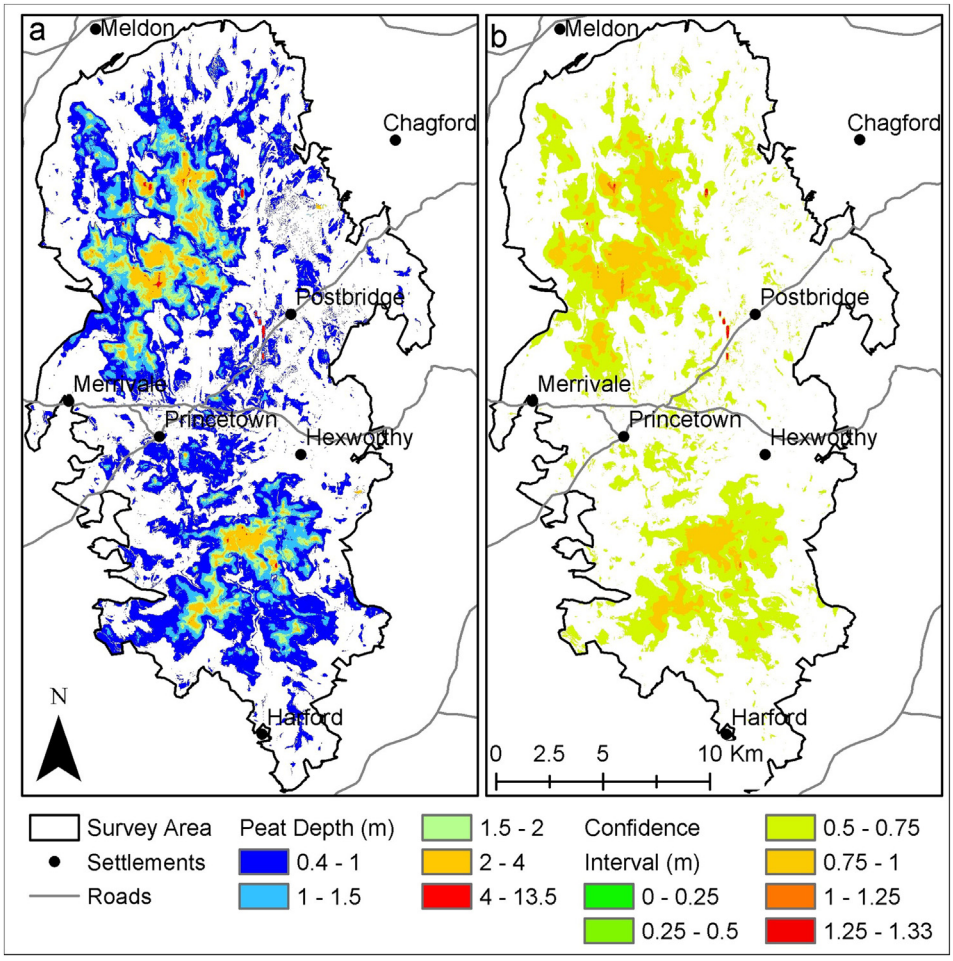

Fig. 4. Modelled peat depth (m) (a) and modelled uncertainty (difference between 5 and 95% confidence interval) (b) both on a linear scale.

Table 3
Estimated peat extent (km^2) and volume (km^3) and peat based carbon (tonnes).

	Mean	5%	95%
Study area			
Area (km^2)	317	213	392
Peat volume (km^3)	0.19	0.12	0.30
Carbon content (Mt C)	15.4	9.6	24.0
Area where peat > 0.4 m			
Area (km^2)	158	99	259
Peat volume (km^3)	0.16	0.10	0.27
Carbon content (Mt C)	13.1	8.1	21.9

saturation. It may be that radiometric dose reflected variation in moisture content but fortuitously there is a functional relationship between moisture content and peat depth.

Using a relationship between peat depth and existing surface conditions, such as moisture content, assumes that current conditions have held over a sufficiently long time to enable a greater depth of peat to accumulate in wet areas. It is most likely that slope is also an indirect measure of surface moisture with greater drainage occurring on steeper slopes. Local variation in peat depth may be more dependent on small scale, often complex, variation in underlying topography (Kettridge et al., 2008) explaining the greater uncertainty in peat depth in areas of peat > 0.7 m (Figs. 3b and 4b). However, the distribution of bog communities has shown a continued dependence on substrate topography (Comas et al., 2004; Graniero and Price, 1999) so underlying topographic features may still be expressed at the surface via varied surface conditions such as moisture content. Other peat depth models (Holden and Connolly, 2011; Parry et al., 2012) similarly found uncertainty in modelled peat depth to increase with peat depth. In addition, in this study, at low radiometric dose values, the signal to noise ratio was lower resulting in increased uncertainty in the radiometric dose value and hence modelled peat depth. Maximum modelled peat depth (13.52 m) is notably greater than the maximum measured peat depth (7.00 m). These high values are due to the logarithmic relationship between radiometric dose and peat depth (Fig. 2d) resulting in a large increase in peat depth for a small decrease in radiometric dose. A maximum limit was considered but its selection would have been arbitrary so it was not used.

Despite these limitations, using radiometric dose together with slope has modelled linear peat depths with a RMSE of 0.31 m and r^2 of 0.66 (RMSE of 0.27 and r^2 of 0.72 for ln scales) over a wide range of peat depths (0 to 7 m), an improvement on previous models. Parry et al. (2012) obtained an r^2 of 0.27 using ln elevation and ln slope to model peat depth across a moorland. They improved the explanatory power of their model to $r^2 = 0.53$ by considering spatial units based on soil and vegetation type separately, consequently this requires some *a priori* knowledge. They obtained a smaller RMSE (0.54 m) for their model however, the range of peat depths covered was smaller (0 to 3.3 m) and deeper peats are associated with greater uncertainty (Holden and Connolly, 2011; Parry et al., 2012 and Figs. 3b and 4). Unlike Parry et al. (2012) who found elevation to be a greater predictor of peat depth than slope, this study found ln slope have a stronger relationship with ln peat depth (Fig. 2a & b) but not as good as ln radiometric dose (Fig. 2d). This difference may be due to the addition of data from Fyfe et al. (2014, 2010) and Harrod (2016) which had a relatively small range in

Table 4
Estimated (Est.), 5 and 95% confidence intervals of peat area (km^2) and carbon stock (tonnes) under land cover types using the radiometric dose and slope model.

Land cover	Total area (km^2)	Area of peat > 40 cm (km^2)			Carbon (Mt C)		
		Est.	5%	95%	Est.	5%	95%
Bog	186.2	96.2	78.7	105.9	9.8	8.7	13.0
Acid grassland	108.4	54.6	20.0	118.3	2.9	1.3	6.9
Improved grassland	7.6	4.5	1.3	16.1	0.2	0.1	0.8
Rough grassland	34.0	1.4	0.4	3.3	0.1	0.0	0.2
Dwarf shrub heath	45.2	6.0	1.7	18.6	0.3	0.1	1.0
Woodland	24.4	2.9	1.0	9.1	0.2	0.7	0.5
Other	12.9	0.5	0.3	1.2	0.0	3.3	0.1

elevation. Rudiyanto et al. (2016) also did not consider slope as a predictor of tropical peat depths, however their survey area was flat compared to Dartmoor (Table 1).

Holden and Connolly (2011) explained up to 63% of the observed variation in peat depth using a topography based model however the resolution was significantly lower (1 km^2) than this study (10 m^2). Using radiometric dose Keaney et al. (2013) modelled peat depths with a correlation coefficient of 0.49 between peat depth and the airborne radiometric data, in this study the inclusion of a topographic metric improved the variability explained. This highlights improved interpretation possible by using data derived from different sources, supplying information on different aspects of the peatland structure and function.

Previous efforts to map peat extents using remotely sensed data have primarily used aerial photography (e.g. Cruickshank and Tomlinson, 1990) or satellite imagery (e.g. Fuller et al., 2002) dependent on the survey area. Similar to Connolly et al. (2007), who found areas mapped as peat to be overlain by non-peat forming vegetation including woodland scrub, natural grasslands and pastures, our study has demonstrated that peat often underlies vegetation types not associated with peat forming conditions (Table 4). This is most likely to occur around the margin of peatlands where land management has altered the vegetation cover, thus breaking the link between peatland vegetation cover and the underlying peat. These areas of relic peat may contain significant carbon stores (Donlan et al., 2016) which are likely to require unique management strategies and have distinct greenhouse gas dynamics (Wilson et al., 2016) due to their differing ecohydrological properties (Schouwenaars, 1993). Whilst all mapping requires ground validation (for both training and testing), the method outlined in this study does not require *a priori* knowledge of land cover and is therefore particularly useful to map relic peats in areas where land management has altered the vegetation cover.

Twenty-eight percent of variability in peat depth remained unexplained by the model, this is most likely due to small scale vertical and horizontal heterogeneity in bedrock radiogenesis, effective water saturation, density and porosity, all of which influence radiometric dose. The peatlands of Dartmoor have a history of peat extraction (Newman, 2010) and currently have extensive systems of peat cuttings, erosional gullies, drainage ditches and bare peat pans (Luscombe et al., 2017) which will have locally affected the hydrology (Connolly et al., 2007; Dixon et al., 2013) and consequently the effective water saturation, density and porosity of the peat. Therefore, the assumption that these properties are constant over the extent of the moor is a known oversimplification.

Radiometric dose measured at the sensor is the result of radiogenesis from the bedrock and attenuation from the overlying soils. Areas of peat consistently show low radiometric doses due to strong attenuation (Beamish, 2013b) however, as radiometric response is broadly governed by the underlying bedrock (Rawlins et al., 2007) it is not possible to derive a single radiometric dose threshold to define peat extent across a range of bedrocks (Beamish, 2015). In this study we restricted the area of interest to overlie granite thereby limiting the variability in bedrock radiogenesis enabling a relationship between radiometric dose and peat depth to be derived. We considered this valid as excluded areas lie away from the high moor where peat formation is less likely. All bedrock materials emit radionuclides which can be monitored by airborne gamma-ray spectrometry. Therefore this method could be widely used, however as the radiometric signal varies with bedrock type (Rawlins et al., 2007) as well as peat depth, to extend this method to other sites with different/mixed bedrock types would require calibration for each bedrock type separately.

Although airborne gamma-ray spectrometric survey data are less commonly available than LiDAR data many modern airborne geophysical datasets exist. The technology is available and could easily be included in future survey flights. In addition, lighter UAV based gamma-ray spectrometers are in development (MacFarlane et al., 2014) which may be deployable to map peat extents and depths in the near future.

4.2. Comparison to existing data

Comparing the mapped extent of peaty soils (Fig. 5, Table 3) to existing maps shows this study estimated a greater area of peat than previously mapped. Winter Hill and Crowdy soil series (National Soil Research Institute, 2018a), both described as blanket peats with peat > 0.4 m, are mapped as covering 115 km^2 of the study area. Although local discrepancies occur, the peat mapped in our study shows moderate agreement (Fig. 5a) with this coarser resolution national survey (kappa = 0.57). Neither map is likely to be completely accurate but compared to the NSI soil map this study obtained a producers accuracy of 87% for peat (> 0.4 m) and 77% for non-peat and users accuracies of 60 and 94% respectively. There are some areas of deep peat in our study which are not mapped as Winter Hill, the thicker of the peat soils units, suggesting that either peat has been overestimated in these areas or incorrectly mapped (Fig. 5a red areas). There are also some deeper peaty soils (> 0.4 m) mapped by our study in areas of Hexworthy and Princetown soil units (Fig. 5a orange areas), both soil units described as peat to loam over granite which contain variable amounts of peat up to 0.4 m.

In contrast the 1:50000 superficial geology map (British Geological Survey, 2016) has a notably smaller area of peat (98 km^2) than this study (Fig. 5b). A large portion of the peat identified by this study on the southern moor, including sampling locations (Fig. 1), have no superficial geology mapped by the BGS (Fig. 5b orange). Some of these areas are mapped as Winter Hill soils (National Soil Research Institute, 2018a), suggesting these areas have been missed out of the BGS superficial map. Particularly in the north of the study area, areas have been mapped by the BGS as peat which have not been mapped by this study (Fig. 5b red). Some discrepancy would be expected as the BGS define peat as a > 1 m thick organic deposit with a readily identifiable margin based on vegetation/soil/topographic change. It is possible the peats to the north of the north moor are thin (< 0.4 m) but due to continuous peatland vegetation cover they have been mapped in continuity with deeper peats.

Parry and Charman (2013) estimated 9.7 ± 2.97 Mt. C within the moorland line of Dartmoor (an area of 471 km^2), which is lower than estimated by this study (13.1 Mt. C, Table 3). For the area with > 0.4 m of peat this study also produces a greater estimate of organic carbon than the NSI soil organic carbon map 3.7 ± 1.4 Mt. C (National Soil Research Institute, 2018b). This is most likely due to greater modelled peat depths in this study, Parry et al.'s (2012) peat depth model predicted a maximum of 3.77 m, the NSI map limited soil depth to 1.5 m (National Soil Research Institute, 2018b), whereas in this study 31 km^2

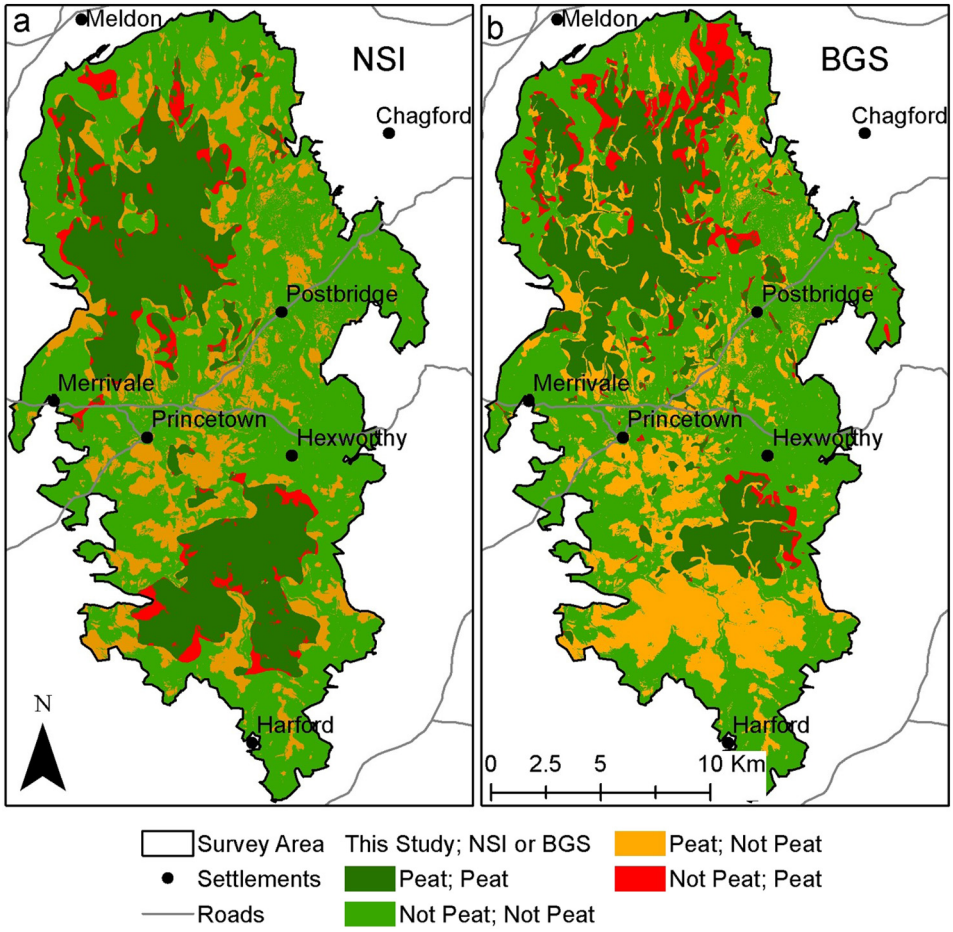

Fig. 5. Modelled peat extent (> 0.4 m) compared to a, the National Soils Institute soil series (© Cranfield University (NSRI) and for the Controller of HMSO [2018]) and b, British Geological Society mapped peat extent (British Geological Survey, 2016).

was mapped as having > 1.5 m of peat and 0.49 km^2 > 4 m. None of these estimates included sub-peat carbon storage, shown to be significant (Fyfe et al., 2014).

5. Conclusions

Peat depth was modelled at a scale useful for land management decisions (10 m^2) across a landscape extent (406 km^2) with a RMSE of only 0.31 m. Mapped peat extents were greater but in broad agreement with previous studies. Estimated carbon stocks were also higher than previous studies mostly due to deeper estimated peat depths in some areas. Combining gamma-ray spectrometric data containing information on soil depth and saturation with LiDAR derived slope, considered a proxy for drainage, has improved upon models using only one of these data sources. Although *a priori* knowledge of bedrock is needed no *a priori* knowledge of land cover was required, therefore this method is particularly useful for identifying relic peats underlying non-peat forming vegetation. These can contain significant carbon stocks which may need tailored management. Some site-specific calibration would be required to allow for variation in bedrock radiogenesis however, this would be undemanding compared to traditional peat depth mapping methods. The inclusion of a gamma-ray spectrometer in future airborne peatland LiDAR surveys is highly recommended due to the increased information content provided.

Acknowledgements

The authors would like to thank the anonymous reviewers for the thorough reviews, their suggestions improved this paper. This work was supported by South West Water [SK06855], Dartmoor National Park Authority [SK07279] and the South West Partnership for Environmental and Economic Prosperity (SWEEP). SWEEP was funded by the Natural Environment Research Council (NE/P011217/1).

Appendix A. Supplementary data

Supplementary data associated with this article can be found in the online version, at doi:https://doi.org/10.1016/j.geoderma.2018.07.041. These data include the Google map of the modelled peat depth (m) described in this article.

References

Aitkenhead, M.J., 2017. Mapping peat in Scotland with remote sensing and site characteristics. Eur. J. Soil Sci. 68, 28–38. https://doi.org/10.1111/ejss.12393.
Akumu, C.E., McLaughlin, J.W., 2014. Modeling peatland carbon stock in a delineated portion of the Nayshkootayaow river watershed in Far North, Ontario using an integrated GIS and remote sensing approach. Catena 121, 297–306. https://doi.org/10.1016/j.catena.2014.05.025.
Avery, B.W., 1980. Soil classification for England and Wales (higher categories). In: Soil Survey of England and Wales, (Harpenden, Technical Monograph No. 14).
Beamish, D., 2013a. Gamma ray attenuation in the soils of Northern Ireland, with special reference to peat. J. Environ. Radioact. 115, 13–27. https://doi.org/10.1016/j.jenvrad.2012.05.031.
Beamish, D., 2013b. Peat mapping associations of airborne radiometric survey data. Remote Sens. 6, 521–539. https://doi.org/10.3390/rs6010521.
Beamish, D., 2015. Relationships between gamma-ray attenuation and soils in SW England. Geoderma 259–260, 174–186. https://doi.org/10.1016/j.geoderma.2015.05.018.
Beamish, D., Howard, A.S., Ward, E.K., White, J., Young, M.E., 2014. Tellus South West Airborne Geophysical Data. Natural Environment Research Council, British Geological Surveyhttps://doi.org/10.5285/73848363-57C1-480A-A64E-

C732E15C4B37. Nat. Environ. Res. Counc. Br. Geol. Surv.
Beilman, D.W., Vitt, D.H., Bhatti, J.S., Forest, S., 2008. Peat carbon stocks in the southern Mackenzie River Basin: uncertainties revealed in a high-resolution case study. Glob. Chang. Biol. 14, 1221–1232. https://doi.org/10.1111/j.1365-2486.2008.01565.x.
Beven, K.J., Kirkby, M.J., 1979. A physically based, variable contributing area model of basin hydrology. Hydrol. Sci. J. 24, 43–69.
Biancalani, R., Avagyan, A., 2014. Towards climate-responsible peatlands management. Mitigation of climate change in agriculture series 9 [WWW Document]. URL. http://www.fao.org/3/a-i4029e.pdf, Accessed date: 1 May 2018.
Bragg, O.M., Tallis, J.H., 2001. The sensitivity of peat-covered upland landscapes. Catena 42, 345–360. https://doi.org/10.1016/S0341-8162(00)00146-6.
British Geological Survey, 2016. 1:50,000 Superficial Geology [Shapefile Geospatial Data], Tiles: EW324 Okehampton, EW325 Exeter, EW337 Tavistock, EW338 Dartmoor, EW339 Newton Abbot, EW349 Ivybridge. [WWW Document]. EDINA Geol. Digimap Serv. < http//edina.ac.uk/digimap > .
Buffam, I., Carpenter, S.R., Yeck, W., Hanson, P.C., Turner, M.G., 2010. Filling holes in regional carbon budgets: predicting peat depth in a north temperate lake district. J. Geophys. Res. 115, G01005. https://doi.org/10.1029/2009JG001034.
Centre for Ecology and Hydrology, 2007. Land Cover Map [Vector Shape geospatial data], Scale 1:2500, Using: EDINA Environment Digimap Service, < http://edina.ac.uk/digimap>, [WWW Document].
Comas, X., Slater, L., Reeve, A., 2004. Geophysical evidence for peat basin morphology and stratigraphic controls on vegetation observed in a Northern Peatland. J. Hydrol. 295, 173–184. https://doi.org/10.1016/J.JHYDROL.2004.03.008.
Comas, X., Terry, N., Slater, L., Warren, M., Kolka, R., Kristiyono, A., Sudiana, N., Nurjaman, D., Darusman, T., 2015. Imaging tropical peatlands in Indonesia using ground-penetrating radar (GPR) and electrical resistivity imaging (ERI): implications for carbon stock estimates and peat soil characterization. Biogeosciences 12, 2995–3007. https://doi.org/10.5194/bg-12-2995-2015.
Connolly, J., Holden, N.M., Ward, S.M., 2007. Mapping peatlands in Ireland using a rule-based methodology and digital data. Soil Sci. Soc. Am. J. 71, 492–499. https://doi.org/10.2136/sssaj2006.0033.
Cruickshank, M.M., Tomlinson, R.W., 1990. Peatland in Northern Ireland: inventory and prospect. Ir. Geogr. 23, 17–30.
Davis, J.L., Annan, A.P., 1989. Ground-penetrating radar for high-resolution mapping of soil and rock stratigraphy. Geophys. Prospect. 37, 531–551. https://doi.org/10.1111/j.1365-2478.1989.tb02221.x.
Dixon, S.D., Qassim, S.M., Rowson, J.G., Worrall, F., Evans, M.G., Boothroyd, I.M., Bonn, A., 2013. Restoration effects on water table depths and CO_2 fluxes from climatically marginal blanket bog. Biogeochemistry 118, 1–18. https://doi.org/10.1007/s10533-013-9915-4.
Donlan, J., Dwyer, J.O., Byrne, K.A., 2016. Area estimations of cultivated organic soils in Ireland: reducing GHG reporting uncertainties. Mires Peat 18, 1–8. https://doi.org/10.19189/MaP.2016.OMB.230.
Erdi-Krausz, G., Matolin, M., Minty, B., Nicolet, J., Redford, W.S., Schetselaar, E.M., 2003. Guidelines for Radioelement Mapping Using Gamma Ray Spectrometry Data. International Atomic Energy Agency.
Ferraccioli, F., Gerard, F., Robinson, C., Jordan, T., Biszczuk, M., Ireland, L., Beasley, M., Vidamour, A., Barker, A., Arnold, R., Dinn, M., Fox, A., Howard, A., 2014. LiDAR Based Digital Surface Model (DSM) Data for South West England. https://doi.org/10.5285/B81071F2-85B3-4E31-8506-CABE899F989A.
Fuller, R.M., Smith, G.M., Sanderson, J.M., Hill, R.A., Thomson, A.G., 2002. The UK Land Cover Map 2000: construction of a parcel-based vector map from satellite images. Cartogr. J. 39, 15–25. https://doi.org/10.1179/caj.2002.39.1.15.
Fyfe, R.M., Woodbridge, J., 2012. Differences in time and space in vegetation patterning: analysis of pollen data from Dartmoor, UK. Landsc. Ecol. 27, 745–760. https://doi.org/10.1007/s10980-012-9726-3.
Fyfe, R.M., Woodbridge, J., Rowe, J., 2010. Archaeological and Palaeoecological Survey at Hangingstone Hill, Winney's Down and Broad Down, Dartmoor. University of Plymouth, Plymouth.
Fyfe, R.M., Coombe, R., Davies, H., Parry, L., 2014. The importance of sub-peat carbon storage as shown by data from Dartmoor, UK. Soil Use Manag. 30, 23–31. https://doi.org/10.1111/sum.12091.
Grand-Clement, E., Anderson, K., Smith, D., Luscombe, D.J., Gatis, N., Ross, M., Brazier, R.E., 2013. Evaluating ecosystem goods and services after restoration of marginal upland peatlands in South-West England. J. Appl. Ecol. 50. https://doi.org/10.1111/1365-2664.12039.
Graniero, P.A., Price, J.S., 1999. The importance of topographic factors on the distribution of bog and heath in a Newfoundland blanket bog complex. Catena 36, 233–254. https://doi.org/10.1016/S0341-8162(99)00008-9.
Harrod, T.R., 2016. Soils in Devon XI Sheet SX68/78 [Mortonhampstead and Chagford] Soil Survey Record No. 117.
Holden, N.M., Connolly, J., 2011. Estimating the carbon stock of a blanket peat region using a peat depth inference model. Catena 86, 75–85. https://doi.org/10.1016/j.catena.2011.02.002.
Householder, J.E., Janovec, J.P., Tobler, M.W., Page, S., Lähteenoja, O., 2012. Peatlands of the Madre de Dios River of Peru: distribution, geomorphology, and habitat diversity. Wetlands 32, 359–368. https://doi.org/10.1007/s13157-012-0271-2.
Joint Nature Conservation Committee, 2011. Towards an assessment of the state of UK Peatlands. JNCC Rep. 445, 77.
Jones, A.M., 2016. Preserved in the Peat: An Extraordinary Bronze Age Burial on Whitehorse Hill, Dartmoor, and its Wider Context. Oxbow, Oxford.
Keaney, A., McKinley, J., Graham, C., Robinson, M., Ruffell, A., 2013. Spatial statistics to estimate peat thickness using airborne radiometric data. Spat. Stat. 5, 3–24. https://doi.org/10.1016/j.spasta.2013.05.003.
Kettridge, N., Comas, X., Baird, A., Slater, L., Strack, M., Thompson, D., Jol, H., Binley, A., 2008. Ecohydrologically important subsurface structures in peatlands revealed by ground-penetrating radar and complex conductivity surveys. J. Geophys. Res. Biogeosci. 113, G04030. https://doi.org/10.1029/2008JG000787.
Lapen, D.R., Moorman, B.J., Price, J.S., 1996. Using ground-penetrating radar to delineate subsurface features along a wetland catena. Soil Sci. Soc. Am. J. 60, 923. https://doi.org/10.2136/sssaj1996.03615995006000030035x.
Lindsay, R., 1995. Bogs: The Ecology, Classification and Conservation of Ombrotrophic Mires. Scottish Natural Heritage, Edinburgh.
Liston-Heyes, C., Heyes, A., 1999. Recreational benefits from the Dartmoor National Park. J. Environ. Manag. 55, 69–80. https://doi.org/10.1006/JEMA.1998.0244.
Luscombe, D.J., Anderson, K., Gatis, N., Wetherelt, A., Grand-Clement, E., Brazier, R.E., 2015. What does airborne LiDAR really measure in upland ecosystems? Ecohydrology 8, 584–594. https://doi.org/10.1002/eco.1527.
Luscombe, D.J., Anderson, K., Grand-Clement, E., Gatis, N., Ashe, J., Benaud, P., Smith, D., Brazier, R.E., 2017. How does drainage alter the hydrology of shallow degraded peatlands across multiple spatial scales? J. Hydrol. 541, 1329–1339. https://doi.org/10.1016/j.jhydrol.2016.08.037.
MacFarlane, J.W., Payton, O.D., Keatley, A.C., Scott, G.P.T., Pullin, H., Crane, R.A., Smilion, M., Popescu, I., Curlea, V., Scott, T.B., 2014. Lightweight aerial vehicles for monitoring, assessment and mapping of radiation anomalies. J. Environ. Radioact. 136, 127–130. https://doi.org/10.1016/j.jenvrad.2014.05.008.
Minty, B.R.S., 1997. Fundamental of airborne gamma-ray spectrometry. AGSO J. Aust. Geol. Geophys. 17, 39–50.
National Soil Research Institute, 2018a. NATMAP Vector, 1:250000 Soil Association Map, http://www.landis.org.uk/data/natmap.cfm [WWW Document]. Landis.
National Soil Research Institute, 2018b. NATMAP Carbon 1:25 000 Soil Organic Carbon Map, http://www.landis.org.uk/data/nmcarbon.cfm. Landis.
Newman, P., 2010. Domestic and Industrial Peat Cutting on North-Western Dartmoor, Devonshire: An Archaelogical and Historical Investigation.
Parry, L.E., 2011. The Sustainable Carbon Management of Moorlands: Spatial Distribution and Accumulation of Carbon on Dartmoor, Southwest England. Coll. Life Environ. Sci. University of Exeter, Exeter.
Parry, L.E., Charman, D.J., 2013. Modelling soil organic carbon distribution in blanket peatlands at a landscape scale. Geoderma 211–212, 75–84. https://doi.org/10.1016/j.geoderma.2013.07.006.
Parry, L.E., Charman, D.J., Noades, J.P.W., 2012. A method for modelling peat depth in blanket peatlands. Soil Use Manag. 28, 614–624. https://doi.org/10.1111/j.1475-2743.2012.00447.x.
Parry, L.E., West, L.J., Holden, J., Chapman, P.J., 2014. Evaluating approaches for estimating peat depth. J. Geophys. Res. Biogeosci. 119, 567–576. https://doi.org/10.1002/2013JG002411.
Parsekian, A.D., Slater, L., Ntarlagiannis, D., Nolan, J., Sebesteyen, S.D., Kolka, R.K., Hanson, P.J., 2012. Uncertainty in peat volume and soil carbon estimated using ground-penetrating radar and probing. Soil Sci. Soc. Am. J. 76, 1911. https://doi.org/10.2136/sssaj2012.0040.
Plado, J., Sibul, I., Mustasaar, M., Jõeleht, A., 2011. Ground-penetrating radar study of the Rahivere peat bog, eastern Estonia. Est. J. Earth Sci. 60, 31–42. https://doi.org/10.3176/earth.2011.1.03.
Rawlins, B.G., Lark, R.M., Webster, R., 2007. Understanding airborne radiometric survey signals across part of eastern England. Earth Surf. Process. Landf. 32, 1503–1515. https://doi.org/10.1002/esp.1468.
Rawlins, B.G., Marchant, B.P., Smyth, D., Scheib, C., Lark, R.M., Jordan, C., 2009. Airborne radiometric survey data and a DTM as covariates for regional scale mapping of soil organic carbon across Northern Ireland. Eur. J. Soil Sci. 60, 44–54. https://doi.org/10.1111/j.1365-2389.2008.01092.x.
Rezanezhad, F., Price, J.S., Quinton, W.L., Lennartz, B., Milojevic, T., Van Cappellen, P., 2016. Structure of peat soils and implications for water storage, flow and solute transport: a review update for geochemists. Chem. Geol. 429, 75–84. https://doi.org/10.1016/j.chemgeo.2016.03.010.
Rudiyanto, Minasny, B., Setiawan, B.I., Arif, C., Saptomo, S.K., Chadirin, Y., 2016. Digital mapping for cost-effective and accurate prediction of the depth and carbon stocks in Indonesian peatlands. Geoderma 272, 20–31. https://doi.org/10.1016/j.geoderma.2016.02.026.
Rudiyanto, Minasny, B., Setiawan, B.I., Saptomo, S.K., McBratney, A.B., 2018. Open digital mapping as a cost-effective method for mapping peat thickness and assessing the carbon stock of tropical peatlands. Geoderma 313, 25–40. https://doi.org/10.1016/J.GEODERMA.2017.10.018.
Schouwenaars, J.M., 1993. Hydrological differences between bogs and bog-relicts and consequences for bog restoration. Hydrobiologia 265, 217–224. https://doi.org/10.1007/bf00007270.
Tallis, J.H., 1997. The southern Pennine experience: an overview of blanket mire degradation. In: Tallis, J.H., Meade, R., Hulme, P.D. (Eds.), Blanket Mire Degradation-Causes, Consequences and Challenges. Proceedings of a Conference at University Of Manchester, 9–11 April 1979. The Macaulay Land Use Research Institute on behalf of the Mires Research Group, Aberdeen, pp. 7–15.
United Nations Framework Convention on Climate Change, 2012. Report of the Conference of the Parties Serving as the Meeting of the Parties to the Kyoto Protocol on its Seventh Session, Held in Durban from 28 November to 11 December 2011. United Nations, Durban.
Wilson, D., Blain, D., Couwenberg, J., Evans, C.D., Murdiyarso, D., Page, S.E., Renou-Wilson, F., Rieley, J.O., Sirin, A., Strack, M., 2016. Greenhouse gas emission factors associated with rewetting of organic soils. Mires Peat 17. https://doi.org/10.19189/MaP.2016.OMB.222.